Open Access

Recent Progress in Materials

LIDSEN Publishing Inc.

Original Research

Enhancing Thermal, Viscoelastic, and Mechanical Properties of Silicone Rubber Matrix through Reinforcements for Use as a Medical Implant

Kianoush Hatami Dehnou, Mohammad Jafar Hadianfard *

Department of Materials Science and Engineering, Shiraz University, Shiraz, Iran; E-Mails: k.hatamidehnou714@gmail.com; hadianfa@shirazu.ac.ir

* **Correspondence:** Mohammad Jafar Hadianfard; E-Mail: hadianfa@shirazu.ac.ir

Academic Editor: Mazen Alshaaer

Special Issue: Synthesis, Characterisation, and Applications of Biomaterials

Recent Progress in Materials
2024, volume 6, issue 2
doi:10.21926/rpm.2402011

Received: December 14, 2023
Accepted: April 22, 2024
Published: May 03, 2024

Abstract

The use of silicone rubber as an implant is limited due to its weak properties. In this study, the impact of various reinforcements, such as TiO_2 or SiO_2 nanoparticles, carbon, or polypropylene fiber micro reinforcements, on the mechanical, thermal, and viscoelastic properties of silicone rubber composites with RTV-4125 matrix was investigated. The composites were evaluated through several tests, including tensile, compression, FTIR, TGA, DMTA, and water adsorption tests. It was found that the composites' tensile strength and compressive stress were increased by adding reinforcements, with the most significant impact on tensile strength observed for SiO_2 and the most notable effect on compressive stress at a strain of 0.5 observed for polypropylene fiber. Moreover, the water absorption of the matrix was increased with the addition of reinforcements, with the highest increase observed for Titania nanoparticles. TGA analysis showed that all composites had higher thermal stability than the plain matrix, with the highest degradation temperature observed for the SR-C fiber composite and the highest degradation rate observed for SR-TiO_2. Additionally, DMTA analysis revealed that TiO_2 nanoparticles considerably decreased the glass transition temperature of the matrix (%28.5), while the other reinforcements had a negligible effect on this temperature. The introduction of reinforcements had a positive impact on the mechanical, thermal, and viscoelastic

properties of silicone rubber composites, and the findings of this study can contribute to the development of new and improved silicone rubber composites for implant applications.

Keywords
Nanoparticles; micro-reinforcement; mechanical properties; thermal; viscoelastic; silicone rubber

1. Introduction

Silicone rubbers are widely used across various fields due to their excellent physical, mechanical, and chemical properties, including low glass transition temperatures, a wide application temperature range, and resistance to ozone and ultraviolet radiation [1]. In the medical industry, silicone rubber has innumerable applications, such as manufacturing medical implants, including finger implants and intervertebral discs for the neck. Additionally, silicone rubber is used in autoclaves to sterilize laboratory tools and equipment [2]. However, silicone rubber's mechanical properties and thermal stability are weaker than other polymers. Therefore, various nano- and micro-reinforcements, such as nanotubes, iron oxides, Nano SiO_2 and TiO_2 particles, and mineral fillers, improve these properties [3].

Considerable efforts have been made to enhance the properties of silicone rubber through various methods. Adding carbon fibers and polypropylene has been considered highly effective, markedly improving silicone rubber's thermal and mechanical properties [4-7]. One of the significant advantages of silicone rubber is its enhanced thermal stability, attributed to the high chemical bond strength of the O-Si-O bond forming the backbone of this polymer [8]. Moreover, the proper dispersion of reinforcement particles with varying sizes in the matrix and the presence of robust covalent bonds in the polymer structure are crucial factors in improving the thermal and mechanical properties of the system [8].

Nanoparticles of SiO_2, when appropriately dispersed in the PFA matrix, along with the reaction between organic and inorganic substances in the material, have been reported to impede the movement of polymer chains during relaxation, thereby increasing the thermal stability of the system [9]. Furthermore, the addition of carbon fibers has been discovered to augment the mechanical strength of silicone rubber, preventing the destruction of silicone rubber chains and, consequently, improving its thermal stability [10].

Recently, the effect of CeO_2 and graphene on the thermal stability of silicone rubber was investigated by Ruigie Han et al. [11]. They observed that the uniform distribution of nanoparticles in the matrix is a crucial factor in determining the properties of the composite. When CeO_2 with appropriate distribution is employed, Ce^{4+} from CeO_2 under thermal oxidation changes to Ce^{3+}, facilitating the free radical scavenging process, preventing the chemical bond breakage of the side group silicone rubber bonds, and improving thermal properties.

The mechanical behavior of matrices has been widely investigated about the influence of nanoparticles. In this regard, TiO_2 particles were analyzed for their effect on the epoxy resin in a study conducted by Vazan et al. [12], which reported an increase in the strength of the material. The effective surface area of mineral fillers has improved through surface modification, leading to a

stronger connection between the reinforcements and the matrix, limiting the movement of polymer chains, and improving thermal and mechanical properties [13]. The strength of silicone rubber was enhanced by modifying the surface of Nano graphene and incorporating it into silicone rubber, as demonstrated by Kumar et al. [14]. In addition, the thermal stability of silicone rubber was observed to increase more effectively with the addition of modified clay than with carbon fiber due to the creation of Si-C bonds, which possess higher strength than C-C bonds [15]. Moreover, the simultaneous addition of iron oxides and carbon nanotubes affected the crystalline structure of γ-Fe_2O_3, an unstable spinel iron oxide, and improved the thermal stability of silicone rubber through CNTs [16]. Proper dispersion and addition of Nano-ribbon graphene significantly affected the mechanical properties and thermal stability of silicone rubber, as reported by Lu Gun et al. [17].

Significant improvements in the mechanical properties of silicone rubber can be achieved by incorporating various additives. Covalent bonds can be formed with the matrix by including SiO_2 nanoparticles, increasing tensile strength and elongation [18]. Similarly, the crosslinking density of silicone rubber can be increased by incorporating palm fibers, resulting in improved strength, elongation, and viscoelastic properties [19]. TiO_2 nanoparticles have also been shown to enhance the mechanical properties and elongation of PLA/SR composites by restricting the movement of polymer chains [20]. Furthermore, water absorption in silicone rubber with different fillers can vary due to differences in the filling of cavities and pores by nanoparticles [21].

Despite extensive research in this area, a comprehensive understanding of the impact of various additives on the properties of different silicone rubbers is still lacking. Therefore, it is essential to gather more information on how different reinforcements affect the behavior and properties of silicone rubber, particularly for various applications. This study investigates the impact of titanium oxide nanoparticles, silicon oxide nanoparticles, carbon, and polypropylene fibers on silicone rubber properties to determine their suitability for cervical intervertebral discs.

2. Materials and Methods

2.1 Materials

The materials used in this research included silicone rubber (RTV-4125), SiO_2 and TiO_2 nanoparticles, Carbon (CF), and Polypropylene (PPF) fibers. Table 1 presents the specific details and specifications of each material. The materials were selected based on their properties and suitability for the intended application.

Table 1 Specifications of Materials.

Specifications / Material	Density (g/cm^3)	Diameter (nm)	Purity (%)	The average length (mm)
Silicone rubber	1.19	-	-	-
TiO_2	4.23	25 (nm)	99.9	-
SiO_2	2.1	15 (nm)	99.9	-
CF	1.9	20 (μm)	99.9	5
PPF	0.9	9 (μm)	99.9	5

2.2 Preparation of Silicone Rubber Composites

Silicone rubber nanocomposites were fabricated by dispersing nanoparticles in 2% acetone by weight. The nanoparticles were then added to silicone rubber and dispersed within the silicone rubber by a mechanical stirrer for 10 minutes. After the acetone was evaporated, the resulting samples were vacuumed to remove any remaining bubbles and then baked at 120°C.

To create silicone rubber fiber composites, 2 volume percent of fibers were added to silicone rubber and dispersed with a mechanical stirrer for 10 minutes. The mixture was then vacuumed to remove bubbles and baked at 120°C. Table 2 presents the sample abbreviations used in this research.

Table 2 samples abbreviation.

abbreviation	Sample
SR	Pure silicone rubber
SR-TiO_2	silicone rubber-2%wt TiO_2
SR-SiO_2	silicone rubber-2%wt SiO_2
SR-C	silicone rubber-2%val CF
SR-PP	silicone rubber-2%val PPF

2.3 Morphology

The distribution of reinforcements in the matrix was investigated by examining the surface of the samples using electron microscopy (SEM) and light microscopy (OM). Before SEM examination, a thin layer of gold was coated on the surface of all specimens (Table 1). The samples were placed under an electron microscope, and the surface morphology was analyzed. The SEM and OM images revealed the matrix's reinforcement distribution.

2.4 Water Absorption

The measurement of water absorption by silicone rubber and its composites followed the ASTM-D570 standard. Samples with specific diameters and thicknesses were cast using pre-made molds. The surface of the samples was then thoroughly cleaned with a clean cloth before being placed in an oven at 120°C for 20 minutes. The samples were subsequently placed in a desiccator until they reached ambient temperature. They were then weighed using a digital scale with an accuracy of 0.001 g. Each sample was floated in deionized water for a week, and every 24 hours, it was removed from the water, dried with a clean cloth, and weighed with the same accuracy. The percentage of water absorption of each sample was then calculated using Equation 1, where W_f is the final weight and W_i is the initial weight of the sample.

$$Water\ absorption = ((W_f - W_i)/W_i) \times 100 \quad (1)$$

2.5 Tensile Test

To determine the tensile properties, according to the ASTM D-412 standard, dumbbell-shaped samples were prepared by employing special molds and subjected to a tensile test at room temperature by a Centam machine with a capacity of 1000 kg and a constant speed of 500 mm/min.

2.6 Compression Test

Compression tests were performed according to the ASTM-D575 standard, and cylindrical samples were prepared and subjected to a compression test by a Centam machine at 12 mm/min.

2.7 FTIR Analysis

To analyze the molecular structure and functional groups in silicone rubber and to investigate the effects of reinforcement additives on these functional groups, infrared spectroscopy on 3 mm thick samples was used. A Bruker-German Tensor II device performed these tests in the range of 400 cm^{-1} to 4000 cm^{-1}.

2.8 Dynamic Mechanical Test

Dynamic mechanical analysis was carried out on plain silicone rubber and silicone rubber composite samples according to the ASTM-D5992 standard to study their viscoelastic behavior. The analysis yielded the elastic modulus (or storage modulus), the viscous modulus (or loss modulus), the damping coefficient, and the glassy temperature, which were determined using the DMA-Trition device manufactured in Germany. The analysis was performed over a temperature range of -150 to +150°C with a heating rate of 5°C/min. The samples used in the analysis were 10 µm thick, 3 cm long, and 1 cm wide.

2.9 TGA Test

A TGA thermal stability analysis was accomplished to investigate the thermal stability of the silicone rubber and the composites. This test was performed under an argon atmosphere by Q600 SDT-TA Instruments. Samples were weighed using Thermo Balance scales in the 5 to 6 mg range, and an alumina crucible was used for heating. In these tests, a heating speed of 10°C/min and a temperature range of 25 to 700°C were selected.

3. Results and Discussions

3.1 FTIR Test

Figure 1 shows the results of the FTIR tests.

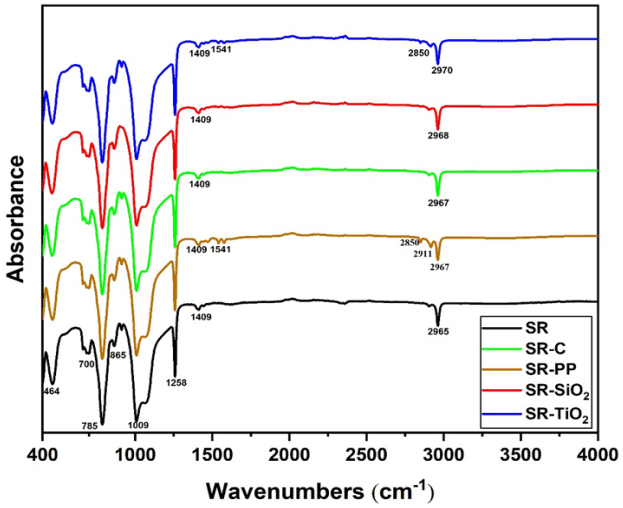

Figure 1 Results of FTIR analysis of silicone rubber and its composites.

Fourier transform infrared (FTIR) spectroscopy was employed to analyze the absorption peaks of the plane sample and composite samples containing various additives to identify any possible changes. The FTIR spectra of the composite samples exhibited modifications to the peaks observed in the plane sample. The 2850 to 2970 cm^{-1} peaks were linked to the tensile vibration of the C-H bond [22]. The peak at 1409 cm^{-1} to 1413 cm^{-1} was associated with the asymmetric tensile vibration of C-H [23]. The Siloxane group was represented by the 460 cm^{-1} to 465 cm^{-1} peaks at 1009 cm^{-1}, signifying the Si-O-Si bond [24]. The peak at 785 cm^{-1} was associated with the $Si(CH_3)_2$ bond, whereas the peaks in the 1258 cm^{-1} to 1270 cm^{-1} range were linked to this bond with lower absorption intensity [25]. The 695 cm^{-1} to 700 cm^{-1} peak was attributed to the Si $(CH_3)_3$ bond.

An increase in adsorption intensity was observed in the peaks at 460, 463, and 1009 cm^{-1} in SR samples with added SiO_2 compared to other additives. The observed increase was attributed to covalent bond formation between silica and silicone rubber facilitated by their similar constituent elements of silicon [24]. A peak at 1541 cm^{-1} was observed in both SR/PP and SR/TiO_2 samples, which was attributed to the forming of an N-H bond by TiO_2 in the presence of UV radiation [26, 27]. Similarly, polypropylene fibers peaked in the range of 1541 cm^{-1} to 1562 cm^{-1} related to the N-H bond. Furthermore, small peaks in the range of 2850 cm^{-1} to 2920 cm^{-1}, related to the C-H bond, were observed and more visible in the SR/PP sample when compared to the other samples. These peaks were removed in the SR/C and SR samples [22, 23]. The findings suggest that SiO_2, PP fibers, and TiO_2 can significantly affect the adsorption intensity of silicone rubber, which may have important implications for various industrial applications. Further research is necessary to understand the full potential of these additives.

The changes observed in the FTIR spectra of the composite samples can be attributed to the interaction between the silicone rubber matrix and the additives. It is known that these changes can affect the mechanical and physical properties of composite materials. Therefore, it is essential to investigate the influence of various additives on the properties of silicone rubber for different applications.

3.2 Morphology

Plain silicone rubber exhibited a transparent color. However, adding nanoparticles to the matrix reduced the silicone rubber's transparency and discoloration. Microstructure analysis, as illustrated in Figure 2 and Figure 3, indicates that the nanoparticles were distributed uniformly throughout the matrix. Nonetheless, micro-aggregates of nanoparticles and voids were also observed, forming when the nanoparticles dispersed and emerged from the surface of the silicone rubber during specimen preparation. SiO_2 nanoparticles, more minor than TiO_2 nanoparticles, demonstrate a higher propensity for particle accumulation, resulting in denser particle distribution and shorter interparticle spacing. Optical microscope images, as shown in Figure 4 and Figure 5, confirm that carbon and polypropylene fibers exhibited good dispersion and adhesion.

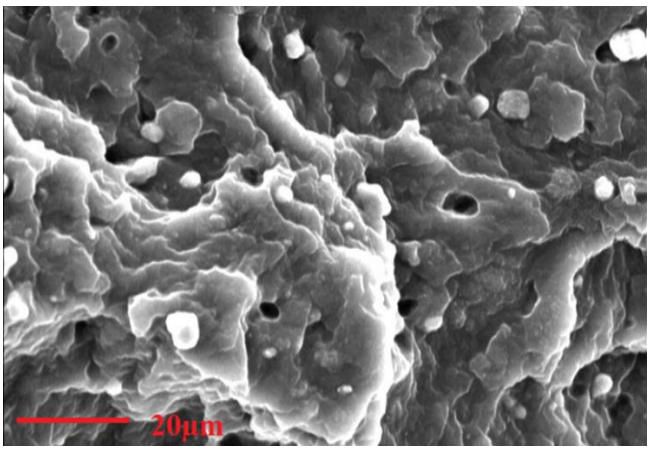

Figure 2 Morphology and microstructure of SR-TiO_2 Nano Composite.

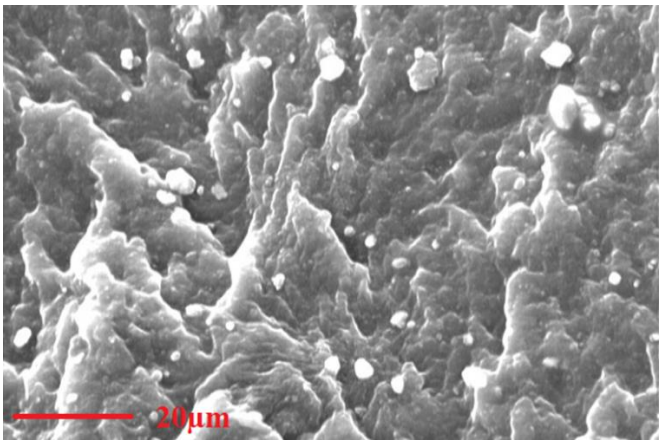

Figure 3 Morphology and microstructure of SR-SiO_2 Nano Composite.

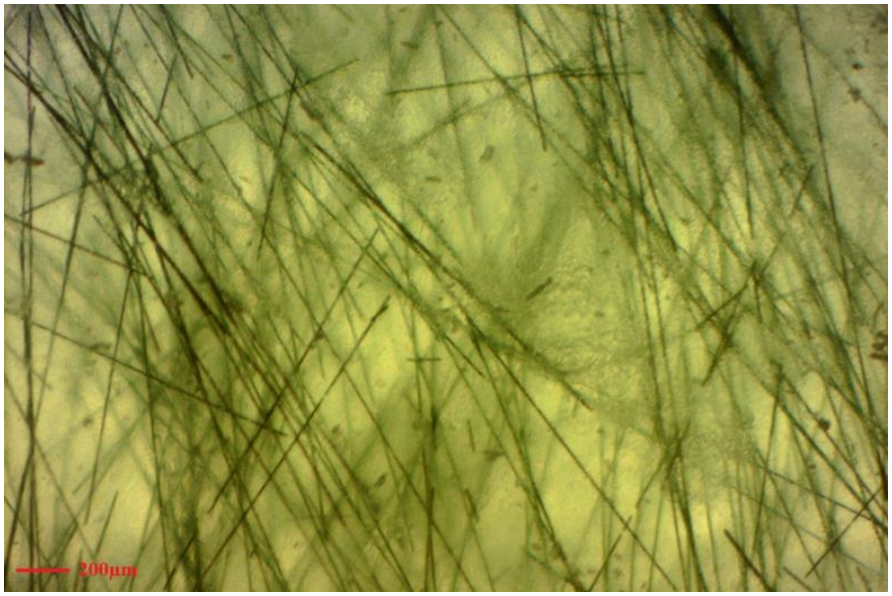

Figure 4 Morphology and microstructure of SR-C Composite.

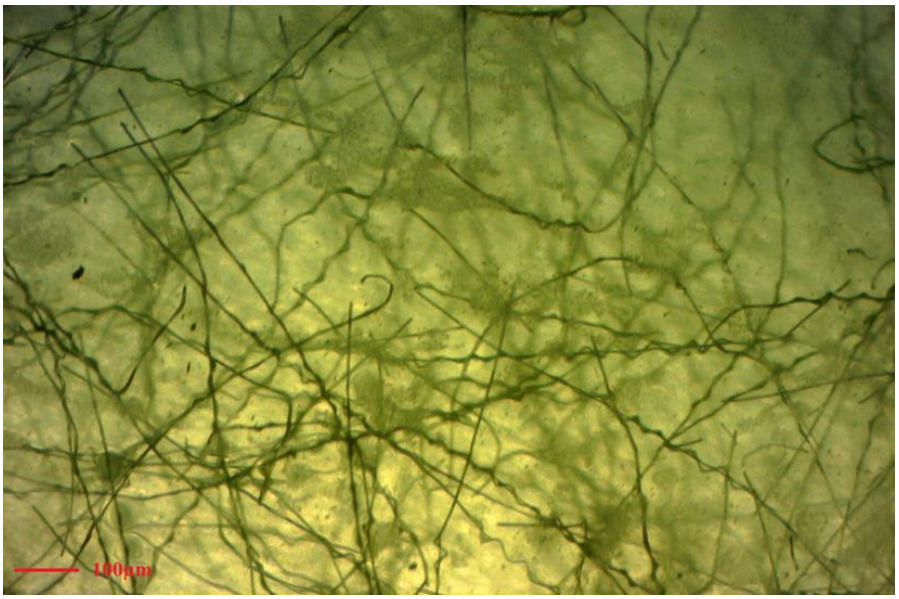

Figure 5 Morphology and microstructure of SR-PP Composite.

3.3 Water Absorption

The percentage of water absorbed by the samples was measured daily for seven days after being placed in distilled water at a temperature of 30°C. The addition of nanoparticles and fibers led to a significant reduction in the amount of water absorption until it reached a constant value, as shown in Figure 6. It was observed that the hydrophobicity of silicone rubber decreased due to the hydrogen atoms in the methyl group located on the surface [28], which reduced the residual energy on the surface of silicone rubber.

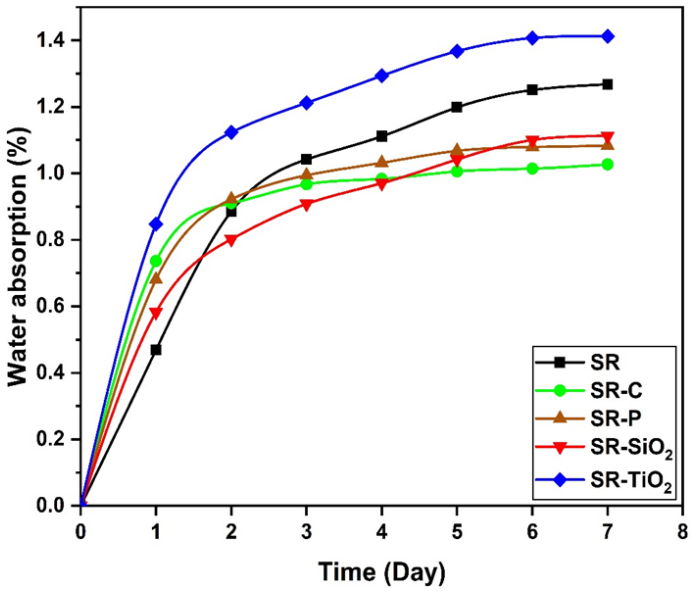

Figure 6 Water absorption of the samples during one-week immersion in distilled water.

Water absorption in materials is influenced by factors such as the presence of voids and porosities that are formed during fabrication. A material's porosity can be reduced by adding reinforcements, including nanoparticles and fibers. The theoretical and practical density measurements and the amount of porosity obtained indicate that the type and size of the reinforcement affect porosity reduction. Polypropylene was the most effective reinforcement in reducing porosity, while TiO_2 had a lower impact than other additives. The results of the water absorption test support these findings. Furthermore, the infrared spectrum analysis of all samples did not reveal the presence of the O-H group, which is known to aid in water absorption (see Figure 7 and Figure 8 for details on theoretical and practical density and porosity measurements).

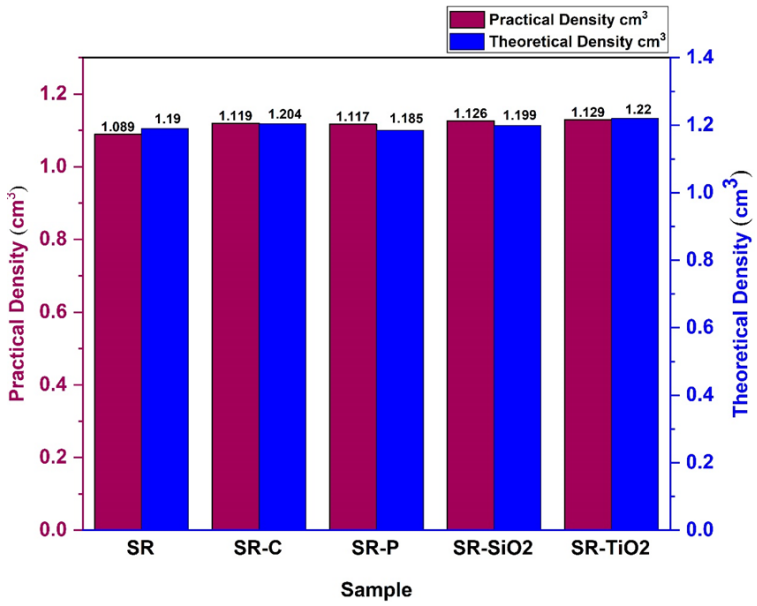

Figure 7 The amount of theoretical and measured density of the samples.

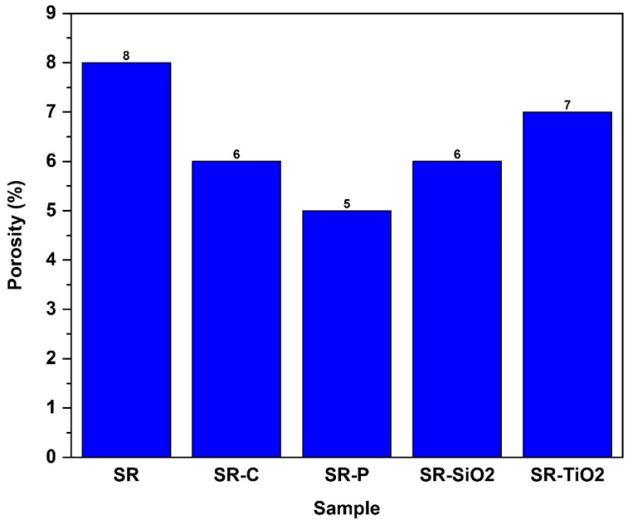

Figure 8 The amount of measured porosity of the samples.

TiO_2 nanoparticles are known to be hydrophilic, resulting in increased water absorption when introduced to a matrix [29]. Polypropylene fibers, being hydrophobic [30], prevent water absorption by the surface molecules of silicone rubber by filling the holes and covering the composite surface. Like polypropylene, carbon fibers cover the composite surface, effectively preventing water absorption. However, carbon fibers have the added benefit of absorbing impurities in water and are therefore used for water purification [31]. Due to the higher density of SR-C compared to SR-PP, water absorption is lower in the SR-C sample than in the SR-PP sample. Additionally, no surface microporosity was observed in either the SR-C or SR-PP samples based on microscopic images.

3.4 Mechanical Properties

3.4.1 Tensile

Figure 9 shows the diagram of stress-strain curves. As seen in Figure 9, the tensile strength of the pure sample is 1.82 MPa, and with the addition of SiO_2 and TiO_2, carbon fibers, and polypropylene fibers, the tensile strength is 7.31, 4.12, 7.23, and 6.88, respectively. MPa is increased. The most significant increase in resistance of almost 300% has been obtained by adding SiO_2 nanoparticles. The effect of SiO_2 nanoparticles in improving resistance is much higher than TiO_2 nanoparticles (300% vs. 126%). Tensile-to-failure measurements were increased in all samples. Due to the increase in length and resistance, the resistance of the samples has also increased. The highest increase in elongation to failure has been measured for carbon fiber (with an increase of 2609%). Adding SiO_2 nanoparticles increased the tensile strength to failure by 2217%. This increase, along with the significant increase in resistance, shows that SiO_2 nanoparticles are a very suitable reinforcement from a mechanical point of view. Carbon fiber has a very high tensile strength due to the C-C bond, which increases its tensile strength when added to polymer materials. According to the figure, tensile strength increased significantly when using carbon fiber.

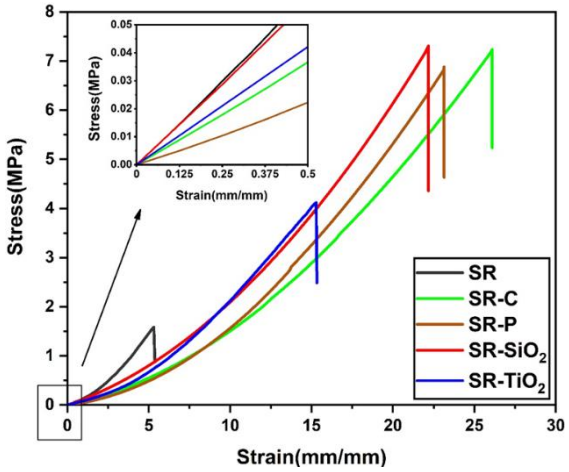

Figure 9 Tensile strength of the composite specimens with various fillers.

The tensile strength in the sample was 7.23 MPa, and the elongation at break increased to 2609%. Also, when using polypropylene fibers as reinforcement, it was observed that the tensile strength reached 6.88 MPa, and the elongation at break reached 2313%. Due to the existence of fibers, the interaction between the field and the fibers has increased and helped to improve the tensile strength. The rubber reinforcement with short fibers includes a combination of the base's elasticity and the fibers' strength and rigidity, and the strength increases with the addition of fibers.

Figure 10 presents the Young's modulus values for all samples. It is observed that Young's modulus decreased in all composites when compared to the pure state, which is consistent with the results obtained by Abdulahi et al. for epoxy resin samples [32]. The decrease in Young's modulus is attributed to the interaction of nanoparticles with the SR polymer chains, which require more tension to open and align the chains. The primary strengthening mechanism in rubber-silicone nanocomposites is attributed to the interactions of the rubber-nanoparticle and nanoparticle-nanoparticle networks [33]. The interactions between rubber and nanoparticles depend on the surface structure and activity of the nanoparticles, leading to the formation of a physical network of rubber nanoparticles, an increase in crosslinking density, or even glassy polymer layers around the nanoparticle surface [34]. The mechanical properties are also likely enhanced due to the covalent bonds between silicone rubber and SiO_2 nanoparticles compared to TiO_2 nanoparticles.

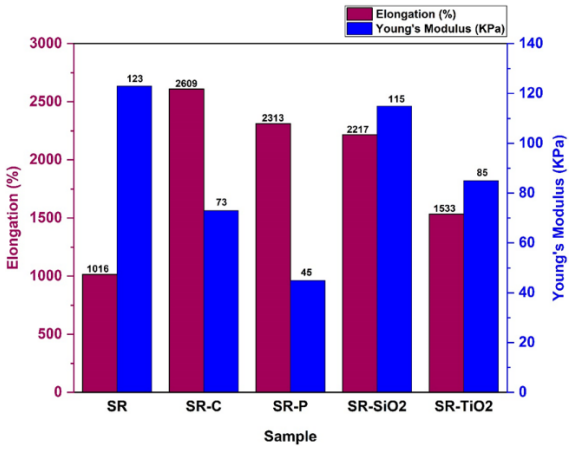

Figure 10 Young's Modulus and Elongation of the composite specimens with various fillers.

The toughness diagram (Figure 11) showed that all the composites exhibited an increase in toughness. The toughness in SR samples, similar to other mechanical properties, increased with reinforcements, allowing for a comparison. The highest toughness among the samples was observed in the SR-C sample, which increased from 7.22 Mj/m^3 to 71.65 Mj/m^3, while the lowest increase was associated with the SR-TiO_2 sample (24.69 Mj/m^3). Among these, both PP and SiO_2 reinforcements significantly contributed to the increase in toughness, with the toughness values of the samples being 57.92 and 62.96 MJ/m^3, respectively.

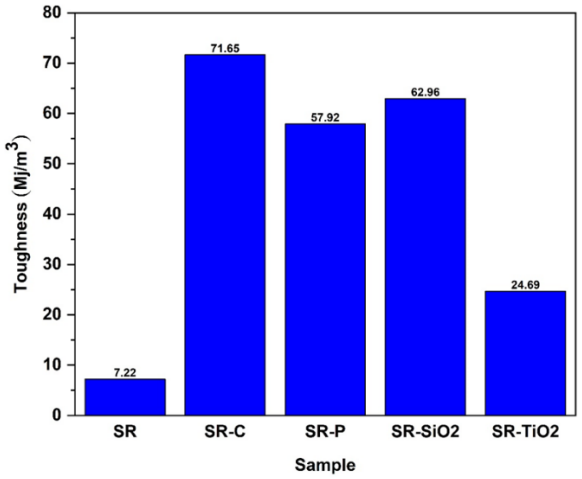

Figure 11 Toughness of the composite specimens with various fillers.

Figure 11 indicates that all composite specimens have considerably higher toughness.

Fibers are commonly used as reinforcements in SR composites because they increase tensile strength and elongation. This property is attributed to the fibers' essential elasticity, strength, and stiffness [35]. Good adhesion between the SR and reinforcements is confirmed by FTIR analysis, which indicates a series of chemical reactions such as N-H, C-H, and Si-O [34]. The presence of agglomerated particles is observed in the SEM images of the fracture surface of the nanocomposites in Figure 2 and Figure 3. However, the series of holes in these images suggests that there is good adhesion between the nanoparticles and SR.

3.4.2 Compressive Tests

Figure 12 illustrates the compressive properties of silicone rubber (SR) and its composites at a strain of 0.5. The pure SR sample exhibits a low compressive strength of 0.65 MPa, significantly improved by adding nanoparticles and fibers. Among the reinforcements, polypropylene (PP) fibers have the most excellent effect, increasing the compressive strength to 1.97 MPa. SiO_2 nanoparticles also exhibit a significant impact, increasing the compressive strength to 1.66 MPa, more substantial than TiO_2 nanoparticles (1.12 MPa) and carbon fibers (1.62 MPa).

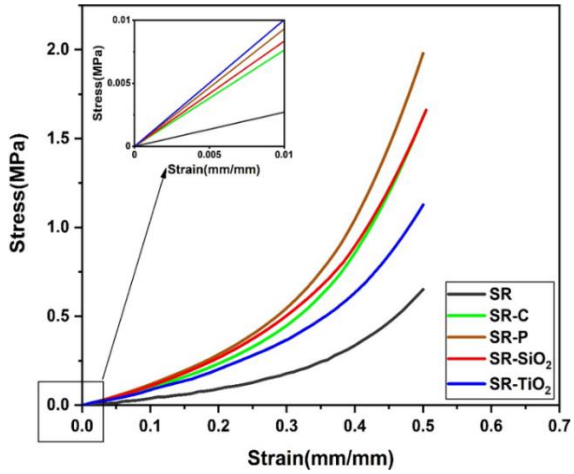

Figure 12 Compressive stress-strain curve of the composite specimens with various fillers.

The increase in compressive strength of the SR-PP composite can be attributed to the transfer of stress from the matrix to fibers with higher strength and modulus. Furthermore, the Poisson effect induces tensile force in the lateral direction, making several fibers oriented perpendicular to the applied pressure. This leads to an increase in compressive stress required for deforming the composite. In contrast to tensile load, where fibers in the direction of applying force have the most significant effect on increasing strength, fibers perpendicular to the direction of applied force have the most significant impact on increasing strength in compression [36].

Nanoparticles in the composites prevent the sliding of polymer chains, thus increasing the compressive stress in the samples. The fibers and the matrix's strength and stiffness significantly influence the samples' compressive properties under load. Adding fibers with higher strength increases the composites' strength due to their superiority over the silicone rubber matrix [37].

Compared to the pure sample, the increase in compressive strength is also attributed to the decrease in porosity and increase in density observed in all the samples (as shown in Figure 7 and Figure 8). The presence of hydrogen bonds, including the N-H bond, may also contribute to the increase in strength, as observed in the FTIR results [38].

3.5 DMTA

This study investigated the dynamic mechanical behavior of silicone rubber and its composites under ambient conditions. The obtained results are presented in Figures 13 to 15, which illustrate the variations of storage modulus (E'), loss modulus (E''), and tangent delta (Tanδ) as functions of temperature for both the plain silicone rubber and composite specimens.

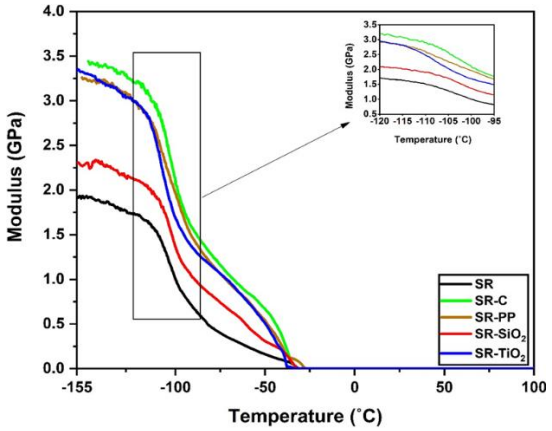

Figure 13 Results of DMTA Analysis -The effect of reinforcements on the Storage Modulus.

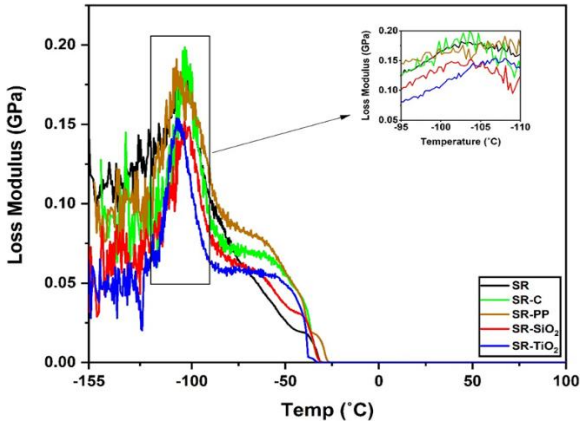

Figure 14 Results of DMTA Analysis -The effect of reinforcements on the Loss Modulus.

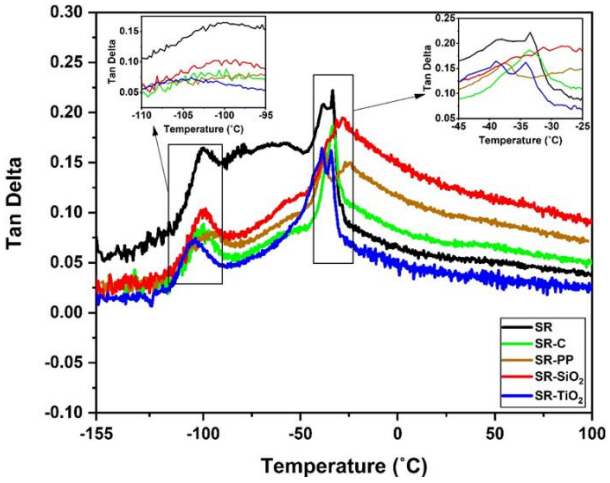

Figure 15 Results of DMTA Analysis -The effect of reinforcements on the damping coefficient.

A transition from the glassy to the rubbery region was observed at low temperatures, leading to a physical softening of the polymer beyond its glass transition temperature (Tg). During this transition, large-scale motion was exhibited by the polymer chains, resulting in a decrease in E', but an increase in E" and Tanδ.

Two distinct transition temperatures, namely, the glass transition temperature and the crystalline melting temperature (Tm), were exhibited by semi-crystalline materials. With increasing temperature, more slip was displayed by the chains at Tm, leading to the crystalline melting stage [39]. As shown in Figure 15, the Tanδ diagram revealed two distinct peaks, one at -100°C corresponding to the glass transition temperature and the other at -33°C corresponding to the crystalline melting temperature.

The dynamic mechanical behavior of silicone rubber and its composites has been investigated to aid in developing advanced materials with tailored mechanical properties. At the glass transition temperature, the mechanical properties of materials can be significantly impacted by the inclusion of nanoparticles and fibers. It has been observed that the presence of these reinforcements results in a reduction of both the damping and dissipation modulus while the storage modulus increases [40, 41]. Moreover, the value of Tanδ slightly shifts towards higher temperatures with the addition of nanoparticles. These results provide valuable insights into the mechanical behavior of silicone rubber and its composites, which can benefit the development of new materials with superior mechanical properties.

It has been observed that the magnitude of change in the storage modulus varies with the type of reinforcement utilized. The highest and lowest amount of change was exhibited by the SR-C and SR-SiO_2 samples, respectively, with their storage moduli increasing from 1.17 GPa to 2.12 and 1.47 GPa [40, 41]. This phenomenon can be attributed to the presence of hydrogen bonds and the effective dispersion of reinforcements within the matrix, as evidenced by microscopic images [40, 41].

The introduction of reinforcement affects composite materials' glass transition temperature (Tg). The reinforcements alter the mechanical properties of the composite material. The Tg of composite materials is generally higher than that of the pure material. The degree of change in Tg varies depending on the type of reinforcement used. The SR-PP and SR-TiO_2 samples exhibit the most significant and least significant changes, respectively. The glass transition temperature of these samples increased from -103°C to -98.85 and -102.37°C, respectively [41].

The effect of reinforcements on the dissipation modulus of composite materials at the glass transition temperature was investigated. The dissipation modulus of the composite materials was lower than that of the pure sample. The SR-SiO_2 sample exhibited the highest reduction in dissipation modulus, while the SR-C sample displayed a minor reduction. Regarding loss modulus, the SR-SiO_2 and SR-C samples decreased from 0.1885 GPa to 0.15284 and 0.13294 GPa, respectively. These results provide insight into modifying composite materials' mechanical and thermal properties by introducing nanoparticles and fibers.

The results demonstrate that adding reinforcements reduces the damping at the glass transition temperature. The SR-SiO_2 sample indicates the highest reduction in damping, while the SR-C sample shows the lowest reduction. The amount of damping for all samples at the glass transition temperature is provided in Table 3. Notably, the composite samples' viscoelastic behavior is almost independent of temperature at the application temperature for the neck disc. This independence can be attributed to silicone rubber's low glass transition temperature. Specifically, it is revealed in Figure 13 that no notable changes in the storage and dissipation modulus or damping coefficient occur at temperatures of approximately -25°C and higher. In conclusion, this study demonstrates that the viscoelastic properties of composite samples at the glass transition temperature can be

significantly affected by the addition of reinforcements. These findings hold implications for the development of enhanced materials for biomedical applications.

Table 3 The Results of DMTA Analysis.

sample	SR	SR-TiO_2	SR-SiO_2	SR-C	SR-PP
Temperature of glass (˚C)	-103	-102.37	-101.35	-100	-98.85
The amount of damping in Tg	0.165	0.103	0.072	0.091	0.087
Percentage of attenuation changes in Tg compared to pure state	-	-37%	-56%	-24%	-47%
The amount of storage modulus in Tg (GPa)	1.17	1.84	1.46	2.12	1.88
Loss modulus value in Tg (GPa)	0.1885	0.14316	0.13294	0.17397	0.15284

3.6 TGA

Figure 16 and Figure 17 exhibit the TGA and DTG analysis of silicone rubber and composites. The samples underwent thermal degradation in three stages, including two main and one primary sub-stage. In the plane sample, a significant reduction in the mass of pure silicone rubber was observed within the temperature range of 320 to 400°C, which can be attributed to a substantial volume of degraded monomers [42].

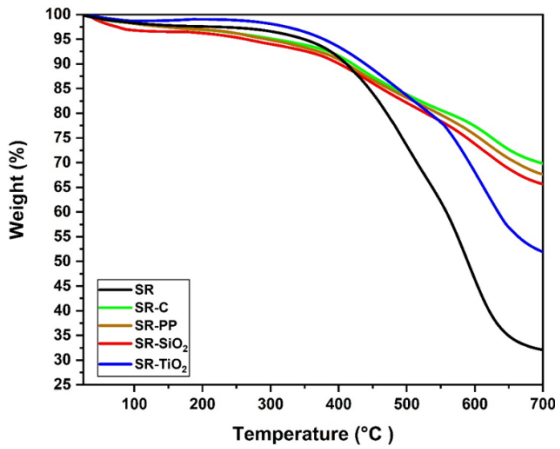

Figure 16 Results of TGA- The effect of reinforcements on the weight reduction of the tested samples due to thermal decomposition.

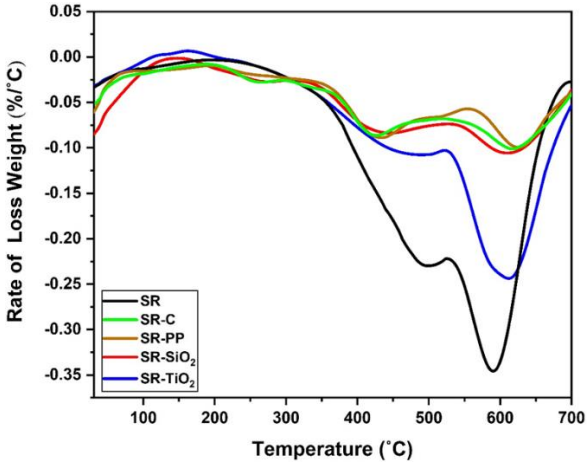

Figure 17 DTG diagram of the composite specimens with various fillers.

The first weight loss stage was observed in all samples within the temperature range of 130 to 260°C, likely due to the evaporation of absorbed moisture and curing agents. The second stage, occurring within the temperature range of 350 to 520°C, is linked to the destruction of silicone rubber networks, resulting in methane production during silicone rubber decomposition [25].

Weight loss in the third stage, within the temperature range of 535 to 680°C, is due to the degradation of small molecular ring siloxane produced during the second stage [3, 43]. The comparison of the TGA diagram of the pure sample with the samples containing reinforcements indicates an upward and rightward shift in the diagrams. This shift suggests a rise in the thermal stability of the composites compared to pure silicone rubber.

The starting temperature of degradation for each sample was recorded, and the results are presented in Table 4. The SR-C sample exhibited the highest increase in starting temperature, rising from 590°C to 625°C, while the SR-SiO_2 sample had the lowest increase, rising to 610°C. The Rmax values for the SR-C and SR-SiO_2 samples decreased from 0.35 (%/˚C) to 0.099 and 0.105 (%/˚C), respectively. The SR-TiO_2 sample showed the highest mass reduction, and the SR-C sample had the lowest. The addition of SiO_2 nanoparticles led to the creation of SiC covalent bonds, which are more potent than silicon chain bonds, resulting in increased thermal stability of the composite [8].

Table 4 Weight change of samples at different temperatures.

Sample	SR	SR-TiO_2	SR-SiO_2	SR-C	SR-PP
T_5(˚C)	347	370	262	291	295
T_{10}(˚C)	410	437	400	410	420
T_{15}(˚C)	444	486	463	468	471
T_{max1}(˚C)	498	490	445	432	425
T_{max2}(˚C)	590	612	610	625	618
R_{max1}(%/˚C)	-0.23	-0.11	-0.084	-0.089	-0.086
R_{max2}(%/˚C)	-0.35	-0.24	-0.105	-0.099	-0.101
Weight changes(%)	68	48.3	34.5	32.5	30.37

The addition of TiO_2 or SiO_2 nanoparticles to silicone rubber creates a type of defect in the arrangement of atoms in the polymer molecules, which restricts the mobility of polymer chains and

results in improved thermal stability of the composite [44]. The absorption of heat by TiO_2 nanoparticles and their prevention of the movement of silicone rubber chains at increased temperatures is attributed to their high thermal conductivity [42]. Additionally, titanium oxide nanoparticles' sizeable active surface area delays the initial decomposition [42].

Adding these nanoparticles creates chemical connection points between the surface of nanoparticles and silicone rubber chains, increasing the crosslinking degree of the polymer [45]. This also leads to the formation of numerous nuclei that enhance the thermal conductivity of materials [8].

Due to crystal defects and atomic vibrations along polymer chains, silicone rubber's weak thermal and mechanical properties can be improved by adding reinforcements such as carbon or polypropylene [46]. The compatibility between fibers and the polymer also reduces weight loss due to heat [47].

The excellent thermal stability of carbon and its outstanding thermal conductivity facilitate heat transfer to the composite when added to silicone rubber. The increased thermal conductivity from adding carbon fiber leads to better heat transfer to the environment [48-51]. By comparing the residual value of the samples at 700°C, it can be concluded that carbon fiber is the best reinforcement for increasing the thermal stability of silicone rubber [48]. Its significant effect on improving the thermal stability of silicone rubber is due to the direct relationship between the residue and thermal stability.

4. Conclusion

This study aimed to investigate the effects of incorporating different reinforcements on the properties of silicone rubber. The mechanical properties of silicone rubber, such as compressive and tensile strength, elongation, and toughness, were enhanced by adding reinforcements. After one week, the water absorption of the samples reached a stable state. Notably, silicone rubber with titanium oxide nanoparticles exhibited higher water absorption than other reinforcements. Furthermore, the thermal properties of silicone rubber were significantly improved. Dynamic mechanical thermal analysis (DMTA) revealed that silicone rubber and other samples remained unchanged when exposed to temperatures above -50°C. The incorporation of reinforcements also improved the thermal stability of silicone rubber. Based on the improved mechanical properties and toughness, reduced water absorption, and the absence of any significant changes in silicone rubber and other samples at temperatures above -50°C, it can be concluded that carbon fibers, polypropylene fibers, and SiO_2 nanoparticles are suitable for manufacturing neck intervertebral discs. However, using TiO_2 nanoparticles is not recommended for cervical intervertebral discs due to their potential to increase the water absorption of silicone rubber.

A proposal for the future could involve research and development in the field of utilizing advanced technologies for implant fabrication using silicone rubber. This includes leveraging innovative manufacturing technologies and improved materials in production processes. Furthermore, further research in the design of silicone rubber structures to enhance the mechanical, thermal, and biological properties of implants could be valuable. Additionally, using advanced research and testing methods, including computer simulations and advanced imaging techniques, could improve the accuracy and validation of silicone rubber implants.

Author Contributions

In this research, Kianoush Hatami Dehnou acted as a postgraduate student. He coordinated and completed all experimental work, participated in data analysis and discussions, and drafted the manuscript. As the supervisor, M.J. Hadianfard was responsible for designing experiments, controlling results, participating in data analysis and discussions, approving conclusions, and finalizing the manuscript.

Competing Interests

The authors have declared that no competing interests exist.

References

1. Cui Y, Yan T, Pan H, Sun H, Bai X, Cao L, et al. Preparation and characterization of intrinsically compatibilized thermoplastic polyurethane and silicone rubber. Macromol Chem Phys. 2022; 223: 2100420.
2. Ziraki S, Zebarjad SM, Hadianfard MJ. On the role of both polypropylene fibers and silica nanoparticles on the viscoelastic behavior of silicone rubber nanocomposites. Polym Plast Technol Eng. 2016; 55: 1693-1699.
3. John Prabhahar M. Role of magnetite (Fe_3O_4)-titania (TiO_2) hybrid particle on mechanical, thermal and microwave attenuation behaviour of flexible natural rubber composite in X and Ku band frequencies. Mater Res Express. 2020; 7: 016106.
4. Zhang H, Yan L, Zhou S, Zou H, Chen Y, Liang M, et al. A comparison of ablative resistance properties of liquid silicone rubber composites filled with different fibers. Polym Eng Sci. 2021; 61: 442-452.
5. Ziraki S, Zebarjad SM, Hadianfard MJ. A study on the tensile properties of silicone rubber/polypropylene fibers/silica hybrid nanocomposites. J Mech Behav Biomed Mater. 2016; 57: 289-296.
6. Azizi S, Momen G, Ouellet-Plamondon C, David E. Enhancement in electrical and thermal performance of high-temperature vulcanized silicone rubber composites for outdoor insulating applications. J Appl Polym Sci. 2020; 137: 49514.
7. Dehnou KH, Norouzi GS, Majidipour M. A review: Studying the effect of graphene nanoparticles on mechanical, physical and thermal properties of polylactic acid polymer. RSC Adv. 2023; 13: 3976-4006.
8. Xu P, Wang H, Tong R, Shen Y, Du Q, Zhong W. A two-dimensional infrared correlation spectroscopic study on the thermal degradation of poly (2-hydroxyethyl acrylate)-co-methyl methacrylate/SiO_2 nanohybrids. Polym Degrad Stab. 2006; 91: 1522-1529.
9. Wang Z, Han E, Ke W. Effect of acrylic polymer and nanocomposite with nano-SiO_2 on thermal degradation and fire resistance of APP-DPER-MEL coating. Polym Degrad Stab. 2006; 91: 1937-1947.
10. Zhang J, Feng S, Ma Q. Kinetics of the thermal degradation and thermal stability of conductive silicone rubber filled with conductive carbon black. J Appl Polym Sci. 2003; 89: 1548-1554.
11. Han R, Wang Z, Zhang Y, Niu K. Thermal stability of CeO_2/graphene/phenyl silicone rubber composites. Polym Test. 2019; 75: 277-283.

12. Wazzan AA, Al-Turaif HA, Abdelkader AF. Influence of submicron TiO_2 particles on the mechanical properties and fracture characteristics of cured epoxy resin. Polym Plast Technol Eng. 2006; 45: 1155-1161.
13. Sarath PS, Thomas S, Haponiuk JT, George SC. Fabrication, characterization and properties of silane functionalized graphene oxide/silicone rubber nanocomposites. J Appl Polym Sci. 2022; 139: e52299.
14. Wang J, Ji C, Yan Y, Zhao D, Shi L. Mechanical and ceramifiable properties of silicone rubber filled with different inorganic fillers. Polym Degrad Stab. 2015; 121: 149-156.
15. Kim ES, Kim EJ, Shim JH, Yoon JS. Thermal stability and ablation properties of silicone rubber composites. J Appl Polym Sci. 2008; 110: 1263-1270.
16. Li H, Tao S, Huang Y, Su Z, Zheng J. The improved thermal oxidative stability of silicone rubber by using iron oxide and carbon nanotubes as thermal resistant additives. Compos Sci Technol. 2013; 76: 52-60.
17. Ou Z, Gao F, Zhao H, Dang S, Zhu L. Research on the thermal conductivity and dielectric properties of AlN and BN co-filled addition-cure liquid silicone rubber composites. RSC Adv. 2019; 9: 28851-28856.
18. Katz S, Lachman N, Hafif N, Rosh L, Pevzner A, Lybman A, et al. Studying the physical and chemical properties of polydimethylsiloxane matrix reinforced by nanostructured TiO_2 supported on mesoporous silica. Polymers. 2022; 15: 81.
19. Bahrain SH, Masdek NR, Mahmud J, Mohammed MN, Sapuan SM, Ilyas RA, et al. Morphological, physical, and mechanical properties of sugar-palm (Arenga pinnata (Wurmb) merr.)-reinforced silicone rubber biocomposites. Materials. 2022; 15: 4062.
20. Mokhtari Aghdami R, Mousavi SR, Estaji S, Dermeni RK, Khonakdar HA, Shakeri A. Evaluating the mechanical, thermal, and antibacterial properties of poly (lactic acid)/silicone rubber blends reinforced with (3-aminopropyl) triethoxysilane-functionalized titanium dioxide nanoparticles. Polym Compos. 2022; 43: 4165-4178.
21. Mehmood B, Akbar M, Ullah R. Water absorption resistance study of HTV silicone rubber-based hybrid composites. Proceedings of the 2021 International Conference on Emerging Power Technologies (ICEPT); 2021 April 10-11; Topi, Pakistan. Piscataway, NJ: IEEE.
22. Rana AS, Vamshi MK, Naresh K, Velmurugan R, Sarathi R. Mechanical, thermal, electrical and crystallographic behaviour of EPDM rubber/clay nanocomposites for out-door insulation applications. Adv Mater Process Technol. 2020; 6: 54-74.
23. Park JJ, Lee JY, Hong YG. Effects of vinylsilane-modified nanosilica particles on electrical and mechanical properties of silicone rubber nanocomposites. Polymer. 2020; 197: 122493.
24. Azizi S, Momen G, Ouellet-Plamondon C, David E. Performance improvement of EPDM and EPDM/silicone rubber composites using modified fumed silica, titanium dioxide and graphene additives. Polym Test. 2020; 84: 106281.
25. Kim HS, Kwon SM, Lee KH, Yoon JS, Jin HJ. Preparation and characterization of silicone rubber/functionalized carbon nanotubes composites via in situ polymerization. J Nanosci Nanotechnol. 2008; 8: 5551-5554.
26. Yuan SJ, Chen JJ, Lin ZQ, Li WW, Sheng GP, Yu HQ. Nitrate formation from atmospheric nitrogen and oxygen photocatalysed by nano-sized titanium dioxide. Nat Commun. 2013; 4: 2249.
27. Hu L, Kang Z. Enhanced flexible polypropylene fabric with silver/magnetic carbon nanotubes coatings for electromagnetic interference shielding. Appl Surf Sci. 2021; 568: 150845.

28. Lin Y, Yin F, Liu Y, Wang L, Zhao Y, Farzaneh M. Effect of ultraviolet-A radiation on surface structure, thermal, and mechanical and electrical properties of liquid silicone rubber. J Appl Polym Sci. 2019; 136: 47652.
29. Xing Y, Lei E, Chen Y, Zhao D, Chang Y, Wang J, et al. Morphological control and hydrophilic properties of TiO_2 nanorod/nanotube films by hydrothermal method. J Electron Mater. 2022; 51: 4565-4579.
30. Xu J, Xin B, Wang C, Zheng Y, Chen C, Zhou M, et al. Tailoring double-layered fibrous mat of modified polypropylene/cotton fabric for the function of directional moisture transport. J Appl Polym Sci. 2020; 137: 49530.
31. Han S, Yang J, Li X, Li W, Zhang X, Koratkar N, et al. Flame synthesis of superhydrophilic carbon nanotubes/Ni foam decorated with Fe_2O_3 nanoparticles for water purification via solar steam generation. ACS Appl Mater Interfaces. 2020; 12: 13229-13238.
32. Abdollahi H, Salimi A, Barikani M, Samadi A, Hosseini Rad S, Zanjanijam AR. Systematic investigation of mechanical properties and fracture toughness of epoxy networks: Role of the polyetheramine structural parameters. J Appl Polym Sci. 2019; 136: 47121.
33. Parvathi K, Bahuleyan BK, Ramesan MT. Optical, thermal and temperature dependent electrical properties of chlorinated natural rubber/copper alumina nanocomposites for flexible electrochemical devices. Res Chem Intermed. 2022; 48: 3897-3914.
34. Idrees M, Saeed F, Amin A, Hussain T. Improvement in compressive strength of styrene-butadiene-rubber (SBR) modified mortars by using powder form and nanoparticles. J Build Eng. 2021; 44: 102651.
35. Kumar RP, Amma MG, Thomas S. Short sisal fiber reinforced styrene-butadiene rubber composites. J Appl Polym Sci. 1995; 58: 597-612.
36. Jawad MK. Investigation of the compression and dielectric strength properties for epoxy/polyurethane blends reinforced with glass fibers. J Al-Nahrain Univ. 2013; 16: 110-114.
37. Salim FM. Analysis of mechanical properties of randomly oriented phenol composites. Diyala J Pure Sci. 2011; 7: 71-85.
38. Wu W, Yu B. The mechanical and thermal properties of KH590-basalt fibre-reinforced silicone rubber/fluorine rubber composites. J Rubber Res. 2020; 23: 163-171.
39. Karami Z, Jazani OM, Navarchian AH, Karrabi M, Saeb MR. Viscoelastic behavior of silicone/clay nanocomposite coatings. Prog Org Coat. 2019; 136: 105214.
40. Lai YH, Kuo MC, Huang JC, Chen M. Thermomechanical properties of nanosilica reinforced PEEK composites. Key Eng Mater. 2007; 351: 15-20.
41. Geng D, Zeng L, Hu B, Li Y, Zhang Y. Dynamic mechanical analysis of nano-SiO_2/bismaleimide composite. Proceedings of the 2008 3rd IEEE International Conference on Nano/Micro Engineered and Molecular Systems; 2008 January 6-9; Sanya. Piscataway, NJ: IEEE.
42. Abdollahi H, Samadi A, Amiri F, Mousapour-Khaneshan V, Zarrintaj P, Kavanlouei M. Kinetics of thermal degradation, adhesion and dynamic-mechanical properties of flexible polyamine-epoxy systems. J Polym Res. 2022; 29: 398.
43. Chandran V, Manvel Ra T, Lakshmanan T, Senthil Kumar M. Influence of different fillers on natural rubber composites to assess mechanical performance. Int J Eng. 2015; 28: 932-939.
44. Wang R, Xie C, Zeng L, Xu H. Thermal decomposition behavior and kinetics of nanocomposites at low-modified ZnO content. RSC Adv. 2019; 9: 790-800.

45. Laachachi A, Ferriol M, Cochez M, Ruch D, Lopez-Cuesta JM. The catalytic role of oxide in the thermooxidative degradation of poly (methyl methacrylate)-TiO_2 nanocomposites. Polym Degrad Stab. 2008; 93: 1131-1137.
46. Ahmadijokani F, Shojaei A, Arjmand M, Alaei Y, Yan N. Effect of short carbon fiber on thermal, mechanical and tribological behavior of phenolic-based brake friction materials. Compos B Eng. 2019; 168: 98-105.
47. Zhao XW, Zang CG, Ma QK, Wen YQ, Jiao QJ. Thermal and electrical properties of composites based on (3-mercaptopropyl) trimethoxysilane-and Cu-coated carbon fiber and silicone rubber. J Mater Sci. 2016; 51: 4088-4095.
48. Yamada S, Serizawa C, Kato K, Yamada S, Serizawa C, Kato K. Thermal and ablative properties of silicone insulation. Proceedings of the 33rd Joint Propulsion Conference and Exhibit; 1997 July 6-9; Seattle, WA, US. Reston, VA: American Institute of Aeronautics and Astronautics (AIAA).
49. Zhu Q, Wang Z, Zeng H, Yang T, Wang X. Effects of graphene on various properties and applications of silicone rubber and silicone resin. Compos Part A Appl Sci Manuf. 2021; 142: 106240.
50. Liu Y, Duan H, Huang Q. Multiscale effect of graphene oxide with short carbon fiber for property improvement of room temperature vulcanized silicone rubber. Polym Bull. 2022; 79: 8471-8485.
51. Azizi B, Rezaee S, Hadianfard MJ, Dehnou KH. A comprehensive study on the mechanical properties and failure mechanisms of graphyne nanotubes (GNTs) in different phases. Comput Mater Sci. 2020; 182: 109794.